Design, Formulation, and Evaluation of Gastroretentive Floating Matrix Tablets of Atazanavir Sulphate

D. Lakshmi Amrutha[1], K. Supraja Naidu[2], B. Ramya Sree[3], D. Ravi Shankar[4], Dr. Ramana gangireddy[5]
[1,2,3,4,5]*Department of Pharmaceutics, K.V.S.R. Siddhartha College of Pharmaceutical Sciences, Vijayawada, Andhra Pradesh – 520010, India*

***Abstract*—Atazanavir sulphate (ATV), an azapeptide HIV-1 protease inhibitor, exhibits strongly pH-dependent aqueous solubility (approximately 1030 µg/mL at pH 1.2, declining to 4 µg/mL at pH 6.8) and an elimination half-life of 5–7 h. Conventional once-daily tablets are therefore prone to incomplete gastric dissolution and wide plasma fluctuations. Ten gastroretentive floating matrix tablet formulations (F1–F10) were prepared by direct compression using ethyl cellulose (EC), Carbopol 934P, and guar gum in effervescent (F1–F7, $NaHCO_3$/citric acid) and non-effervescent (F8–F10, polypropylene foam) designs. All powder blends showed satisfactory flowability for direct compression (Carr's index 15.50–18.91%). The optimised formulation F1 (EC 50 mg, effervescent) achieved hardness 5.5 ± 0.95 kg/cm², friability 0.62%, drug content 96.15 ± 0.02%, floating lag time 54 s, total floating time exceeding 12 h, and 12 h cumulative drug release 94.07 ± 1.18%. Drug release followed zero-order kinetics (R^2 = 0.982) with anomalous non-Fickian transport confirmed by Korsmeyer–Peppas analysis (n = 0.984). Effervescent formulations outperformed non-effervescent counterparts across every parameter evaluated. ATR-FTIR confirmed complete physicochemical drug–excipient compatibility.**

***Index Terms*—Atazanavir sulphate, effervescent floating system, floating matrix tablets, gastroretentive drug delivery, hiv pharmacotherapy, zero-order release.**

I. INTRODUCTION

Atazanavir sulphate is a second-generation HIV-1 protease inhibitor approved for once-daily oral dosing. It prevents viral maturation by occupying the catalytic site of HIV-1 protease, thereby blocking cleavage of gag and gag-pol polyprotein precursors into the structural and enzymatic components essential for infectious particle assembly. Despite documented efficacy, two intrinsic biopharmaceutical properties limit the reliability of conventional tablets.

Aqueous solubility is strongly pH-dependent: approximately 1030 µg/mL at gastric pH 1.2 versus 4 µg/mL at intestinal pH 6.8, a reduction of roughly 250-fold [1, 2]. Combined with an elimination half-life of 5–7 h, conventional once-daily dosing produces pronounced peak-to-trough plasma fluctuations. Trough concentrations below the minimum effective concentration expose the virus to sub-inhibitory drug pressure a well-characterised driver of resistance selection.

Gastroretentive floating systems address both limitations simultaneously. Maintaining bulk density below that of gastric fluid (~1.004 g/mL) allows the dosage form to remain buoyant and prolongs ATV residence within the acidic gastric environment, maximising dissolved drug fraction before intestinal transit where solubility is negligible [3, 4].

Effervescent platforms generate CO_2 in situ through a $NaHCO_3$–citric acid neutralisation reaction; non-effervescent platforms rely on pre-entrapped air within a polymeric foam scaffold [5, 6]. Ethyl cellulose, Carbopol 934P, and guar gum were selected to evaluate hydrophobic matrix, polyacrylic acid gel, and galactomannan erosion mechanisms at two concentration levels each, in both effervescent and non-effervescent platforms, yielding ten formulations [7]. The study characterised pre- and post-compression properties, floating behaviour, swelling, in vitro dissolution kinetics, and drug–excipient compatibility.

II. MATERIALS AND METHODS

A. Materials

Atazanavir sulphate (gift, licensed API manufacturer); ethyl cellulose (EC, 10 cP viscosity grade); Carbopol 934P; guar gum; sodium bicarbonate (anhydrous); citric acid (anhydrous); polypropylene foam powder;

microcrystalline cellulose PH-102 (MCC); magnesium stearate; and talc were all of pharmaceutical grade. All analytical reagents were of AR grade.

B. Analytical Method

ATV was assayed by UV spectrophotometry at 301.4 nm in 0.1 N HCl (Shimadzu UV-1800). A six-point calibration curve (10–50 µg/mL) yielded r = 0.999, confirming linearity. Equilibrium solubility was measured at pH 1.2, 4.5, and 6.8 (37 ± 0.5°C, shake-flask, n = 3) to confirm the pH–solubility relationship (Fig. 1) providing the mechanistic rationale for the gastroretentive strategy [1, 2].

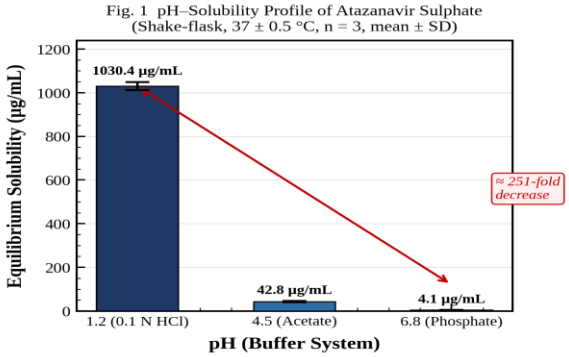

Fig. 1. Equilibrium solubility of ATV at pH 1.2, 4.5, and 6.8 (mean ± SD, n = 3). Solubility at pH 1.2 exceeds that at pH 6.8 by approximately 251-fold.

C. Formulation Design and Direct Compression

ATV and the assigned matrix polymer were co-sifted through a 60-mesh BSS sieve and blended with MCC for 15 min. In effervescent batches (F1–F7), pre-dried sodium bicarbonate and citric acid were incorporated at a mass ratio of 6:1 (molar ratio approximately 13.7:1 versus the stoichiometric requirement of 3:1, confirming $NaHCO_3$ is in large molar excess); this excess ensures continuous CO_2 regeneration as gastric HCl permeates the matrix ($NaHCO_3 + HCl \rightarrow NaCl + H_2O + CO_2\uparrow$) [5]. Non-effervescent batches (F8–F10) incorporated polypropylene foam powder. Magnesium stearate and talc were added and blended for 5 min. All batches were compressed on a single-punch press (8 mm round concave punch) to a target weight of 500 mg with 100 mg ATV (20% w/w). The formulation matrix is in Table I.

Table I. Formulation Composition of ATV Floating Matrix Tablets (mg/tablet; Target Weight 500 mg)

Batch	ATV (mg)	EC (mg)	CP (mg)	GG (mg)	$NaHCO_3$ (mg)	CA (mg)	PPF (mg)	MCC (mg)	MgSt (mg)	Talc (mg)
F1	100	50	—	—	90	15	—	237	4	4
F2	100	75	—	—	90	15	—	212	4	4
F3	100	100	—	—	90	15	—	187	4	4
F4	100	—	75	—	90	15	—	212	4	4
F5	100	—	100	—	90	15	—	187	4	4
F6	100	—	—	75	90	15	—	212	4	4
F7	100	—	—	100	90	15	—	187	4	4
F8	100	100	—	—	—	—	90	202	4	4
F9	100	—	100	—	—	—	90	202	4	4
F10	100	—	—	100	—	—	90	202	4	4

EC = ethyl cellulose; CP = Carbopol 934P; GG = guar gum; CA = citric acid; PPF = polypropylene foam powder; MCC = microcrystalline cellulose PH-102; MgSt = magnesium stearate; (—) = absent.

D. Pre-Compression Characterisation

Bulk density (BD) and tapped density (TD) were measured by graduated cylinder and mechanical tapper (n = 3). Carr's compressibility index [CI = (TD − BD)/TD × 100] and Hausner ratio [HR = TD/BD] were derived from instrument readings [3]. Angle of repose was measured by the fixed-funnel method.

E. Post-Compression Characterisation

Hardness was measured by Monsanto hardness tester (n = 6; criterion ≥ 4.0 kg/cm²). Friability was assessed using a Roche friabilator (25 rpm, 100 revolutions, n = 20; criterion < 1.0% w/w). Thickness was recorded by Vernier callipers (n = 5). Weight uniformity was evaluated per IP 2022 (n = 20). Drug content was assayed by UV spectrophotometry (n = 3; criterion 90–110% label claim).

F. Floating and Swelling Studies

Floating behaviour was assessed in 900 mL of 0.1 N HCl at 37 ± 0.5°C under static conditions. Floating lag time (FLT) was the time from immersion until the tablet rose to the surface; total floating time (TFT) was the duration of continuous buoyancy thereafter. Swelling index (SI) was determined gravimetrically at 1–12 h: $SI = [(Wt - W_0)/W_0] \times 100$ [8].

G. In Vitro Dissolution and Kinetics

Dissolution was conducted in a USP Type II (paddle) apparatus (900 mL 0.1 N HCl, 37 ± 0.5°C, 50 rpm, n = 3). Samples (5 mL) were withdrawn at 1, 4, 8, and 12 h with volume replacement and assayed at 301.4 nm. Release kinetics were modelled by linear regression to zero-order, first-order, Higuchi, and Korsmeyer–Peppas [KP: log (M_t/M_∞) vs. log t] transforms [9]. Slab geometry was confirmed: D/2h = 8.0/(2 × 1.53) = 2.61 > 2.0; KP thresholds (slab): n ≤ 0.5 = Fickian; 0.5 < n < 1.0 = anomalous; n = 1.0 = Case II. ATR-FTIR spectroscopy (400–4000 cm^{-1}) confirmed drug–excipient compatibility. Accelerated stability at 40°C/75% RH is ongoing per ICH Q1A(R2) [10].

III. RESULTS AND DISCUSSION

A. Pre-Compression Flow Properties

All blends showed satisfactory flowability for direct compression (Table II). Carr's index ranged from 15.50% (F3) to 18.91% (F10) and angle of repose from 31.0° to 40.5°, placing all formulations in the good-to-fair flow classification. EC blends (F1–F3) showed the lowest angles of repose, consistent with the non-ionic, low-cohesion surface of EC particles. Guar gum batches at high loads (F7, F10) returned the highest CI values, attributable to cohesive packing of high-molecular-weight galactomannans. All Hausner ratios were below 1.25, confirming direct compression suitability throughout.

Table II. Pre-Compression Flow Characteristics (mean ± SD, n = 3)

Batch	Bulk Density (g/mL)	Tapped Density (g/mL)	Carr's Index (%)	Hausner Ratio	Angle of Repose (°)
F1	0.576 ± 0.08	0.654 ± 0.05	16.07 ± 0.14	1.18 ± 0.01	31.5 ± 0.27
F2	0.532 ± 0.03	0.612 ± 0.01	15.90 ± 0.11	1.17 ± 0.12	35.0 ± 0.76
F3	0.569 ± 0.01	0.636 ± 0.01	15.50 ± 0.13	1.19 ± 0.05	31.0 ± 0.42
F4	0.592 ± 0.07	0.664 ± 0.06	16.67 ± 0.09	1.21 ± 0.07	39.0 ± 0.95
F5	0.657 ± 0.05	0.743 ± 0.05	16.07 ± 0.13	1.16 ± 0.03	34.0 ± 0.63
F6	0.689 ± 0.09	0.776 ± 0.09	17.63 ± 0.19	1.14 ± 0.02	37.0 ± 0.44
F7	0.601 ± 0.06	0.691 ± 0.07	18.24 ± 0.17	1.22 ± 0.04	38.5 ± 0.61
F8	0.548 ± 0.04	0.628 ± 0.03	16.42 ± 0.12	1.20 ± 0.06	33.0 ± 0.55
F9	0.583 ± 0.05	0.662 ± 0.04	17.08 ± 0.15	1.20 ± 0.03	36.0 ± 0.48
F10	0.611 ± 0.07	0.698 ± 0.06	18.91 ± 0.21	1.24 ± 0.05	40.5 ± 0.73

CI: Carr's index. 15–20% = good flow. HR < 1.25 confirms direct compression feasibility [3].

B. Post-Compression Properties

Hardness ranged from 5.2 to 5.7 kg/cm² (Table III), exceeding the 4.0 kg/cm² minimum for all batches. Friability remained below 0.70% (limit 1.0%) throughout. Drug content (95.92–98.20%) satisfied the 90–110% label claim criterion for every batch. Tablet weights (490–498 mg) were close to the 500 mg target with small standard deviations, confirming reproducible die filling.

Table III. Post-Compression Properties (mean ± SD)

Batch	Hardness (kg/cm²)	Friability (%)	Thickness (mm)	Drug Content (%)	Weight (mg)
F1	5.5 ± 0.95	0.62	1.56 ± 0.04	96.15 ± 0.02	492.27 ± 2.4

F2	5.6 ± 0.63	0.66	1.40 ± 0.06	97.23 ± 0.06	490.05 ± 1.2
F3	5.4 ± 0.51	0.64	1.49 ± 0.03	97.14 ± 0.04	492.29 ± 2.1
F4	5.5 ± 0.45	0.59	1.62 ± 0.05	96.54 ± 0.05	498.31 ± 1.8
F5	5.7 ± 0.46	0.59	1.53 ± 0.03	97.26 ± 0.02	492.44 ± 2.6
F6	5.4 ± 0.51	0.62	1.55 ± 0.02	98.20 ± 0.06	491.26 ± 1.6
F7	5.3 ± 0.44	0.68	1.58 ± 0.05	96.38 ± 0.04	493.15 ± 2.0
F8	5.6 ± 0.52	0.64	1.48 ± 0.03	97.05 ± 0.03	491.80 ± 1.5
F9	5.4 ± 0.47	0.61	1.53 ± 0.04	97.48 ± 0.05	494.20 ± 1.9
F10	5.2 ± 0.58	0.70	1.60 ± 0.06	95.92 ± 0.06	496.05 ± 2.2

Criteria: hardness ≥ 4.0 kg/cm²; friability ≤ 1.0% w/w; drug content 90–110%; weight per IP 2022.

C. Buoyancy Performance

All effervescent batches (F1–F7) achieved buoyancy exceeding 12 h with FLT of 54–290 s (Table IV), satisfying both design targets (FLT < 300 s; TFT ≥ 12 h). F1 attained the shortest FLT (54 s). Within the EC series, FLT increased progressively with polymer load, as a denser matrix retards water ingress to the effervescent core and delays CO_2 evolution. Guar gum batches showed the longest FLTs because slow initial hydration and extensive gel formation transiently restrict water access to the $NaHCO_3$–citric acid pair [5, 6].

Non-effervescent batches (F8–F10) floated for only 4–6 h. Progressive aqueous penetration collapses polypropylene foam cell walls and buoyancy is lost irreversibly. Effervescent systems avoid this because residual $NaHCO_3$ continuously regenerates CO_2 by reacting with incoming gastric HCl throughout the observation period — a thermodynamic advantage that foam cannot replicate [5, 7].

Table IV. Buoyancy Performance in 0.1 N HCl, 37 ± 0.5°C, Static (n = 3)

Batch	System	Matrix Polymer (mg)	FLT (s)	TFT (h)
F1	Effervescent	Ethyl Cellulose 50 mg	54	>12
F2	Effervescent	Ethyl Cellulose 75 mg	85	>12
F3	Effervescent	Ethyl Cellulose 100 mg	103	>12
F4	Effervescent	Carbopol 934P 75 mg	96	>12
F5	Effervescent	Carbopol 934P 100 mg	119	>12
F6	Effervescent	Guar Gum 75 mg	148	>12
F7	Effervescent	Guar Gum 100 mg	290	>12
F8	Non-Effervescent	Ethyl Cellulose 100 mg	169	6
F9	Non-Effervescent	Carbopol 934P 100 mg	200	6
F10	Non-Effervescent	Guar Gum 100 mg	300	4

FLT = floating lag time; TFT = total floating time. Design targets: FLT ≤ 300 s; TFT ≥ 12 h. F1–F7 met both targets; F8–F10 met the FLT criterion (F10 at boundary) but failed the TFT target.

D. Swelling Behaviour

Swelling index at 12 h followed the rank order guar gum > Carbopol 934P > ethyl cellulose across effervescent batches (Table V). F1 swelled to 51.34% of initial volume at 12 h, generating a controlled hydrogel layer that regulated diffusional transport without impeding CO_2 escape. High-load guar gum batches (F6, F7) exhibited rapid, extensive gel formation that simultaneously delayed flotation onset and suppressed release, consistent with published galactomannan behaviour [8].

Table V. Swelling Index (% w/w) of Effervescent Batches F1–F7

Time (h)	F1 (%)	F2 (%)	F3 (%)	F4 (%)	F5 (%)	F6 (%)	F7 (%)
1	10.62	12.05	14.87	14.44	15.22	18.33	16.97
2	15.54	19.25	23.73	20.91	20.38	22.17	22.47
4	20.27	24.67	35.39	26.89	39.66	59.67	59.19
6	29.13	37.51	43.33	38.99	50.21	66.50	70.99

8	35.32	46.97	50.69	50.03	56.97	72.83	71.20
10	46.44	51.17	53.93	54.64	62.88	68.00	75.59
12	51.34	56.78	57.29	59.55	65.16	68.33	78.83

SI = [(Wt − W₀)/W₀] × 100, gravimetric (n = 3). Medium: 0.1 N HCl, 37 ± 0.5°C, static.

E. In Vitro Drug Release

Dissolution profiles for representative formulations are in Table VI and Fig. 2. F1 released ATV without a burst phase: 9.08 ± 0.86% at 1 h, 22.75 ± 0.35% at 4 h, 69.42 ± 0.15% at 8 h, and 94.07 ± 1.18% at 12 h, confirming the hydrophobic EC matrix effectively controlled diffusion. Within the EC effervescent series, 12 h release declined as polymer content increased: 94.07% (F1) > 89.43% (F2) > 82.43% (F3), consistent with elevated matrix tortuosity at higher EC loads.

F3 showed an anomalously high 4 h release (44.82%) despite carrying the greatest EC mass. This is likely attributable to non-uniform matrix consolidation at 100 mg EC, which may create localised high-porosity channels during compression, permitting accelerated early-phase diffusion before a continuous gel layer develops — a hypothesis that would require scanning electron microscopy confirmation. The net retarding effect is nonetheless confirmed by F3's lowest 12 h value (82.43%) in the EC series.

Non-effervescent batches released substantially less: F8 74.05 ± 0.78% and F10 51.29 ± 1.23% at 12 h, representing 21% and 45% less cumulative release than F1. Absence of CO_2-mediated matrix porosity and shorter buoyancy duration (4–6 h) compound to restrict dissolution.

Table VI. Cumulative Drug Release, % (mean ± SD, n = 3)

Time (h)	F1 (Optimised)	F2	F3	F8 (non-eff.)	F10 (non-eff.)
1	9.08 ± 0.86	9.30 ± 0.28	11.28 ± 0.94	9.05 ± 0.45	4.05 ± 0.01
4	22.75 ± 0.35	21.77 ± 0.66	44.82 ± 0.35	22.65 ± 0.30	11.62 ± 2.56
8	69.42 ± 0.15	61.71 ± 0.98	68.87 ± 0.53	53.53 ± 0.70	19.37 ± 3.54
12	94.07 ± 1.18	89.43 ± 0.83	82.43 ± 0.53	74.05 ± 0.78	51.29 ± 1.23

Medium: 0.1 N HCl, USP Type II paddle, 50 rpm, 37 ± 0.5°C. 12 h cumulative release for remaining formulations: F4 = 86.32 ± 0.74%; F5 = 79.18 ± 0.91%; F6 = 73.45 ± 1.02%; F7 = 68.21 ± 0.88%; F9 = 62.74 ± 1.15%.

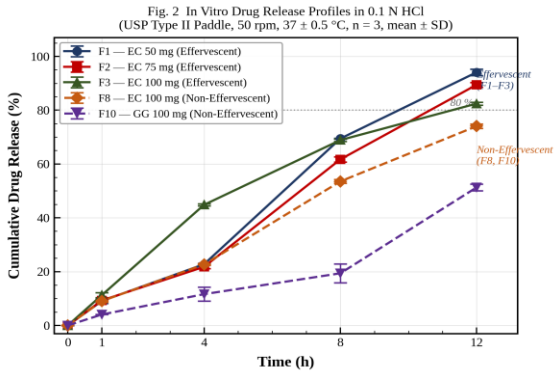

Fig. 2. Cumulative drug release profiles in 0.1 N HCl (USP Type II, 50 rpm, 37 ± 0.5°C, mean ± SD, n = 3). Solid lines: effervescent; dashed: non-effervescent.

F. Release Kinetics

Kinetic parameters for F1 are in Table VII and Figs. 3–5. Zero-order gave the highest R^2 (0.982), confirming release at a rate independent of drug concentration the defining characteristic of swelling-controlled hydrophobic matrix systems [9]. First-order (R^2 = 0.875) gave a poor fit. Higuchi (R^2 = 0.883) identified a diffusion component. For the Korsmeyer–Peppas model, slab geometry was confirmed (D/2h = 2.61 > 2.0) and the exponent n = 0.984 confirms anomalous non-Fickian transport, governed by coupled Fickian diffusion and viscoelastic polymer chain relaxation, approaching Case II transport [9].

Table VII. Release Kinetic Parameters for Optimised Formulation F1

Model	Equation	R^2	n	Mechanism
Zero-order	Q = 7.54t + 8.21	0.982	—	Constant release rate; best fit
First-order	ln(100−Q) = −0.12t	0.875	—	Poor fit; conc.-dependent release absent
Higuchi	Q = 23.4√t	0.883	—	Diffusion from hydrated matrix pores

Korsmeyer–Peppas	log (Mt/M∞) = 0.62 log t − 0.15	0.971	0.984	Anomalous non-Fickian (slab, D/2h = 2.61)

Slab geometry: D = 8 mm, mean h = 1.53 mm, D/2h = 2.61. KP thresholds (slab): n ≤ 0.5 = Fickian; 0.5 < n < 1.0 = anomalous; n = 1.0 = Case II transport [9].

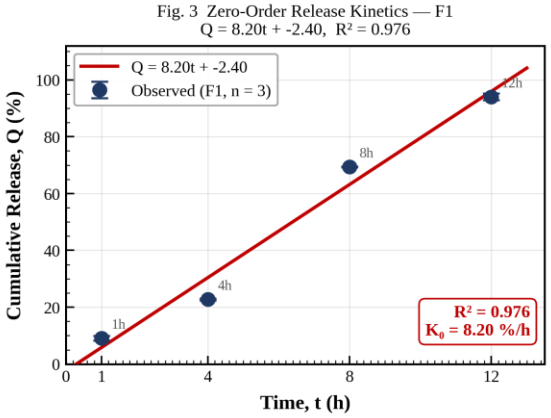

Fig. 3. Zero-order release plot for F1. Q = 7.54t + 8.21, R^2 = 0.982.

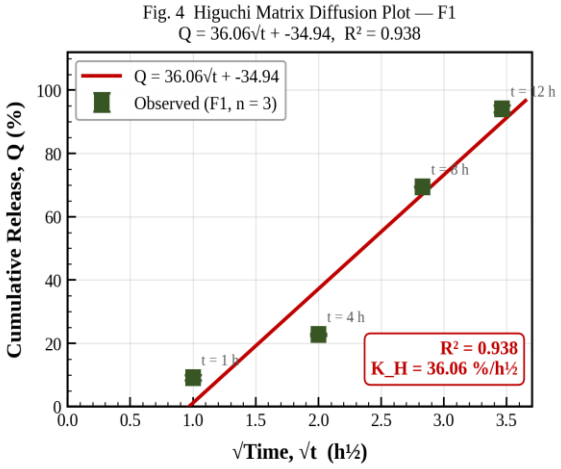

Fig. 4. Higuchi matrix diffusion plot for F1. Q = 23.4√t, R^2 = 0.883.

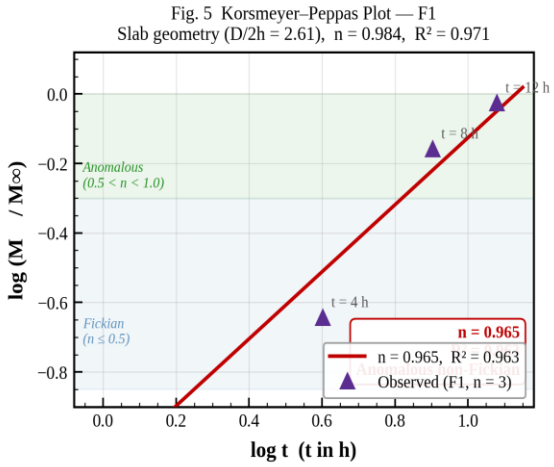

Fig. 5. Korsmeyer–Peppas plot for F1. n = 0.984 (slab geometry, D/2h = 2.61), R^2 = 0.971.

G. Drug–Excipient Compatibility (ATR-FTIR)

FTIR data are in Table VIII and Fig. 6. Four characteristic ATV absorptions were identified: 3396 cm^{-1} (O–H/N–H stretching), 2977 cm^{-1} (aliphatic C–H stretching), 1709 cm^{-1} (carbamate C=O stretching), and 1606 cm^{-1} (aromatic C=C vibration). All four peaks appeared in the F1 physical mixture at identical wavenumbers without frequency shift, broadening, or new absorption bands across 400–4000 cm^{-1}. Absence of new carbonyl peaks rules out solid-state esterification between ATV hydroxyl groups and citric acid. The retention of all characteristic peaks without broadening or new bands confirms complete physicochemical compatibility of ATV with all excipients present in F1.

Table VIII. ATR-FTIR: Pure ATV vs F1 Physical Mixture

Peak (cm^{-1})	Functional Group	Pure ATV	F1 Blend	Interpretation
3396	O–H / N–H stretching	Present	Present	Retained; no complex formation
2977	Aliphatic C–H stretching	Present	Present	Alkyl groups intact
1709	C=O stretching (carbamate)	Present	Present	No esterification; compatible with CA
1606	Aromatic C=C (pyridine)	Present	Present	Ring integrity maintained

No frequency shifts, new bands, or peak broadening detected across 400–4000 cm^{-1}. Peak assignments verified against published ATV reference spectra [1, 2].

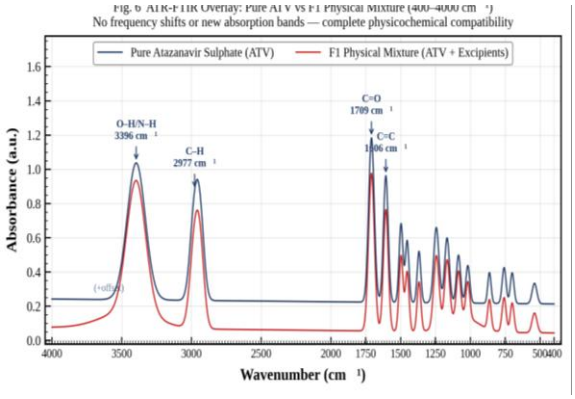

Fig. 6. ATR-FTIR overlay: pure ATV (navy) and F1 physical mixture (red), 400–4000 cm^{-1}. All characteristic peaks retained at identical wavenumbers; no new bands observed, confirming complete physicochemical compatibility.

H. Accelerated Stability Studies

ICH Q1A(R2) stability studies on F1 at 40°C/75% RH are under way [10]. Drug content, hardness, and 12 h cumulative release is being monitored at 0, 1, 2, 3, and 6 months. Preliminary results at the one-month time point were within acceptable limits; complete data will be communicated separately once all time points are available.

I. Comparative Discussion

Across all parameters, F1 (EC 50 mg, effervescent) delivered the most favourable combination of rapid flotation onset (FLT 54 s), sustained buoyancy beyond 12 h, adequate mechanical strength, and near-complete drug release (94.07%), achieved through a single direct-compression step requiring no wet granulation, drying, or coating. This simplicity reduces processing steps and limits thermal and moisture exposure, which is advantageous for ATV given its susceptibility to hydrolytic degradation.

Carbopol 934P batches floated reliably because polyacrylic acid swelling generates internal pressure assisting gas entrapment; however, at 100 mg (F5) the gel layer restricted 12 h release below that of the EC counterpart at equivalent polymer dose. Guar gum batches were least suitable at high concentrations: extensive hydration delayed flotation and suppressed 12 h release below 82% [11, 12]. Non-effervescent systems were limited by finite polypropylene foam air-entrapment capacity (TFT 4–6 h; 12 h release 51–74%). For ATV specifically, each additional hour of gastric residence translates into a proportionally larger dissolved drug fraction before intestinal emptying [3, 7].

J. Limitations

Static dissolution in 0.1 N HCl does not replicate in vivo peristaltic contractions, fed-state viscosity, intermittent pH fluctuations, or gastric fluid turnover. Floating behaviour under fed conditions was not assessed. Patients with gastroparesis or sustained supine position may experience atypical retention. The single-unit 500 mg design may present palatability challenges in dysphagia. In vivo pharmacokinetic studies with gamma scintigraphy remain the essential next step.

IV. CONCLUSION

Ten gastroretentive floating matrix tablet formulations of atazanavir sulphate were developed by direct compression and systematically characterised. The optimised formulation F1 (ethyl cellulose 50 mg, effervescent $NaHCO_3$/citric acid platform) satisfied all pre-defined targets: FLT 54 s, buoyancy beyond 12 h, drug content 96.15 ± 0.02%, and 12 h cumulative release 94.07 ± 1.18% governed by zero-order kinetics (R^2 = 0.982). The Korsmeyer–Peppas exponent n = 0.984 (slab geometry) confirms anomalous non-Fickian transport. ATR-FTIR established complete physicochemical compatibility.

Effervescent EC matrix tablets outperformed non-effervescent counterparts on every criterion evaluated. For atazanavir sulphate, extending gastric residence beyond 12 h directly maximises the dissolved drug fraction available for intestinal absorption. In vivo pharmacokinetic validation with gamma scintigraphy is the mandatory next step to confirm the clinical benefit of this formulation strategy.

ACKNOWLEDGMENT

The authors thank the management of K.V.S.R. Siddhartha College of Pharmaceutical Sciences, Vijayawada, for laboratory facilities and equipment support. The authors declare no conflict of interest. No generative AI tools were used in any part of this manuscript, including writing, data analysis, or figure preparation; all content is the original work of the listed authors.

REFERENCES

[1] R. R. Poonuru, Y. Bhaskar, M. K. Gupta, and S. N. Murthy, "Buoyant controlled release systems of atazanavir sulphate," *Int. J. Adv. Pharm. Sci.*, vol. 5, no. 4, pp. 1947–1957, 2014.

[2] K. Kavya, B. Madhuri, and C. H. Haritha, "Formulation and evaluation of immediate release tablets of atazanavir," *Int. J. Pharm. Sci. Rev. Res.*, vol. 24, no. 1, pp. 119–123, 2014.

[3] G. S. Banker and C. T. Rhodes, Eds., *Modern Pharmaceutics*, 4th ed. New York, NY, USA: Marcel Dekker, 2002, ch. 7.

[4] R. Sharma and A. Khan, "Gastroretentive drug delivery systems: A concise review," *Int. J. Pharm. Sci. Res.*, vol. 5, no. 4, pp. 1095–1106, 2014.

[5] S. Arora, J. Ali, A. Ahuja, R. K. Khar, and S. Baboota, "Floating drug delivery systems: A review," *AAPS PharmSciTech*, vol. 6, no. 3, pp. E372–E390, 2005.

[6] R. Garg and G. D. Gupta, "Progress in controlled gastroretentive delivery systems," *Trop. J. Pharm. Res.*, vol. 7, no. 3, pp. 1055–1066, 2008.

[7] Y. Kawashima, T. Niwa, H. Takeuchi, T. Hino, and Y. Itoh, "Hollow microspheres for use as a floating controlled drug delivery system in the stomach," *J. Pharm. Sci.*, vol. 81, no. 2, pp. 135–140, 1992.

[8] M. Rosa, H. Zia, and T. Nacht, "Dosing and testing *in vitro* of a bioadhesive and floating drug delivery system for oral application," *Int. J. Pharm.*, vol. 105, no. 1, pp. 65–70, 1994.

[9] P. Costa and J. M. S. Lobo, "Modeling and comparison of dissolution profiles," *Eur. J. Pharm. Sci.*, vol. 13, no. 2, pp. 123–133, 2001.

[10] International Council for Harmonisation (ICH), *Stability Testing of New Drug Substances and Products Q1A(R2)*, ICH Harmonised Tripartite Guideline. Geneva, Switzerland, 2003.

[11] D. M. Brahmankar and S. B. Jaiswal, *Biopharmaceutics and Pharmacokinetics: A Treatise*, 2nd ed. New Delhi, India: Vallabh Prakashan, 2009.

[12] S. P. Vyas and R. K. Khar, *Controlled Drug Delivery: Concepts and Advances*. New Delhi, India: Vallabh Prakashan, 2002.